Journal of Quantitative Spectroscopy & Radiative Transfer 203 (2017) 530–537

Contents lists available at ScienceDirect

Journal of Quantitative Spectroscopy & Radiative Transfer

journal homepage: www.elsevier.com/locate/jqsrt

The CO_2 absorption continuum by high pressure CRDS in the 1.74 μm window

D. Mondelain [a,b,*], A. Campargue [a,b], P. Čermák [a,b,c], R.R. Gamache [d], S. Kassi [a,b], S.A. Tashkun [e,f], H. Tran [g]

[a] Univ. Grenoble Alpes, LIPhy, F-38000 Grenoble, France
[b] CNRS, LIPhy, F-38000 Grenoble, France
[c] Department of Experimental Physics, Faculty of Mathematics, Physics and Informatics, Comenius University, Mlynská dolina F2, 842 48 Bratislava, Slovakia
[d] Department of Environmental, Earth, and Atmospheric Sciences, University of Massachusetts, Lowell, MA, USA
[e] Laboratory of Theoretical Spectroscopy, V.E. Zuev Institute of Atmospheric Optics, Siberian Branch, Russian Academy of Sciences,1, Academician Zuev Square, 634055 Tomsk, Russia
[f] Laboratory of Climate and Environmental Physics, Ural Federal University, Mira street, 19, Yekaterinburg 620002, Russia
[g] Laboratoire de Météorologie Dynamique, IPSL, CNRS UMR 8539, Sorbonne Universités, UPMC Univ. Paris 06, 75252 Paris, France

ARTICLE INFO

Article history:
Received 24 January 2017
Received in revised form
27 February 2017
Accepted 28 February 2017
Available online 1 March 2017

Keywords:
Carbon dioxide
CO_2
Transparency windows
Venus
Continuum

ABSTRACT

The very weak absorption continuum of CO_2 is studied by Cavity Ring Down Spectroscopy in three 20 cm^{-1} wide spectral intervals near the centre of the 1.74 μm window (5693–5795 cm^{-1}). For each spectral interval, a set of room temperature spectra is recorded at pressures between 0 and 10 bar thanks to a high pressure CRDS spectrometer. The absorption continuum is retrieved after subtraction of the contributions due to Rayleigh scattering and to local lines of CO_2 and water (present as an impurity in the sample) from the measured extinction. Due to some deficiencies of the CO_2 HITRAN2012 line list, a composite line list had to be built on the basis of the Ames calculated line list with line positions adjusted according to the Carbon Dioxide Spectroscopic Databank and self-broadening and pressure shift coefficients calculated with the Complex Robert Bonamy method. The local line contribution of the CO_2 monomer is calculated using this list and a Voigt profile truncated at ± 25 cm^{-1} from the line centre. Line mixing effects were taken into account through the use of the impact and Energy Corrected Sudden approximations.

The density dependence of the retrieved continuum absorption was found to be purely quadratic in the low frequency interval below 5710 cm^{-1} but a small significant linear contribution was required to reproduce the observations above this value. This linear increase is tentatively attributed to the foreign-continuum of water vapor present in CO_2 sample with a relative concentration of some tens ppm.

The retrieved binary coefficient is observed to vary smoothly with the wavenumber with a minimum value of 6×10^{-10} cm^{-1} $amagat^{-2}$. By gathering the present data with the results reported in *Kassi* et al. *J Quant Spectrosc Radiat Transf 2015;167:97*, a recommended set of binary coefficients is provided for the 5700–5950 cm^{-1} region.

1. Introduction

With a relative concentration of about 96.5%, carbon dioxide strongly dominates the absorption spectrum of Venus and only a restricted number of narrow near infrared (NIR) windows between 0.8 and 2.5 μm can be used to sound the deep atmosphere and the surface. These windows correspond to regions of low opacity between the strong absorption bands of carbon dioxide. They are of importance for the determination of the concentrations of many trace gasses like CO, H_2O, HDO, CO, OCS, SO_2, HF and HCl in different altitude ranges [1]. The 1.74 μm window, for example, provides information on H_2O and HCl mole fraction in the 15 to 30 km altitude range [1]. In these windows, the main contributions to gaseous absorption are due to a local lines (LL) contribution (pressure-broadened) and the so-called "continuum" absorption (CA) slowly varying with frequency. This latter includes absorption due to the transient dipole induced during inter-molecular collisions (or Collision-Induced Absorption, CIA) [2,3] and the far wings of allowed nearby CO_2 bands [4]. Various analyses of the Venus night side have shown that CA is a major contributor to the gas opacity in the

* Corresponding author at: Université Grenoble Alpes Pôle Phitem Laboratoire LIPhy CS 40 700 38058 Grenoble Cedex 9.
E-mail address: didier.mondelain@univ-grenoble-alpes.fr (D. Mondelain).

http://dx.doi.org/10.1016/j.jqsrt.2017.02.019
0022-4073/

windows. To model the spectra recorded with ground-based instruments and on board satellite platforms like the Venus Express spacecraft, spectroscopic databases like CDSD [5] and HITEMP [6] are used to calculate the local lines contribution. Note that the LL contribution in the region of the absorption bands was recently investigated experimentally and theoretically over a broad spectral range (600–9650 cm^{-1}) and up to pressures close to the liquefaction conditions [7,8]. Contrary to the relatively well-characterized LL opacity, the CA is mostly unknown and generally modeled with a constant value over a window with no temperature dependence [9–11]. The absence of laboratory measurements for pressure and temperature conditions relevant for Venus [12] (i.e. from 175 K and 26 μbar at 100 km altitude to 735 K and 92 bar at the surface) makes necessary to adjust the CA level to better reproduce the recorded spectra. As a result, the uncertainty on the CA in the windows leads to significant uncertainties on the retrieved mixing ratios of water vapor in Venus atmosphere. For example in the 1.18 μm window, a 40% uncertainty on the CO_2 continuum absorption adds a ± 3 ppm uncertainty on the H_2O mixing ratio which represents 6.7% of the retrieved mixing ratio [13].

Due to the difficulty of determining broad and weak absorption signal windows, only a few laboratory determinations of CA of CO_2 in the NIR have been reported so far, all at room temperature. In the 2.1 μm window, Tonkov et al. reported measurements for pressures in the 10 –50 atm range using different Fourier transform and grating spectrometers [4]. In the 1.75 and 1.18 μm windows, the continuum is weaker and its detection made necessary to develop high sensitivity laser spectrometers coupled with high pressure cells. The CA in the 1.18 μm window has been determined by Snels et al. with a high pressure Cavity Ring Down Spectrometer (CRDS) [14]. We used the same technique described in [15] to characterize the CA in the high energy edge of the 1.74 μm window (5850–5960 cm^{-1}) from CRDS spectra recorded up to 10 amagat. At 2.1 μm, the high sensitivity of the CRDS technique allowed us to determine the CO_2 CA from spectra recorded at sub-atmospheric pressures [16].

The aim of the present work is to extend the spectral coverage of the 1.74 μm window by high pressure CRDS in the region of lowest opacity between 5693 and 5795 cm^{-1} (see Fig. 1). The experimental set-up is briefly described in Part 2 together with the spectra calibration. The available databases of CO_2 transitions in the region were found insufficient to account for the recorded CRDS spectra and an improved CO_2 database had to be constructed

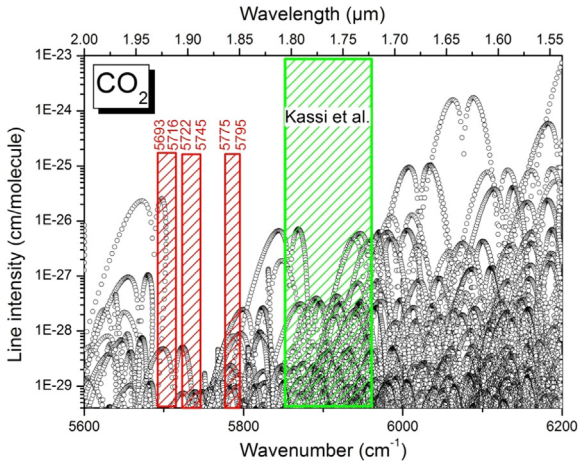

Fig. 1. Overview of the CDSD [5] line list of carbon dioxide in the 1.74 μm window. The three regions dashed in red correspond to the spectral ranges investigated in this work while the green light dashed region highlights the 5850–5960 cm^{-1} interval studied in Ref. [15]. (For interpretation of the references to color in this figure legend, the reader is referred to the web version of this article.)

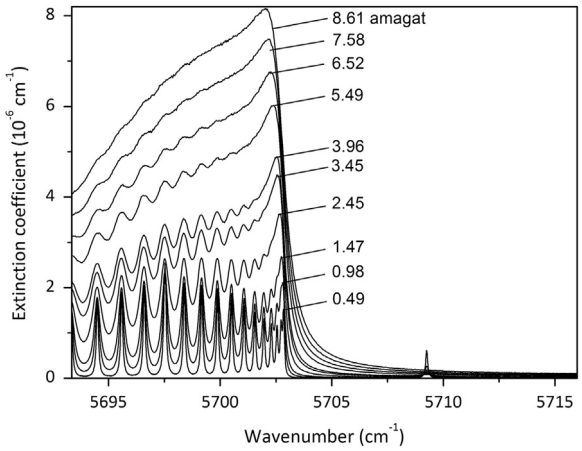

Fig. 2. Overview of the series of pure CO_2 spectra recorded at different densities in the region of R branch of the 00031–10002 band.

in order to satisfactorily subtract the LL contribution. The construction of the LL database and the continuum retrieval with the derivation of the binary coefficients are detailed in Part 3 and Part 4, respectively. Finally, the results and their uncertainty are discussed in Part 5.

2. Experimental set-up and spectra calibration

2.1. High pressure CRDS

The high pressure CRDS cell was previously described in details (see Fig. 2 of Ref. [15]). Briefly, two high reflectivity mirrors are placed on both sides of a stainless steel tube (cavity length of 128 mm) with one of the mirror mounted on a piezo electric transducer (PZT). To strictly avoid perturbations of the optical alignment by pressure forces, this pre-aligned CRDS cavity is inserted into a high pressure cell consisting of a cylinder closed by two thick wedged glass windows. Several holes are drilled in the tube constituting the high finesse cavity (HFC) to allow pressure equilibrium on both sides of the mirrors when the cylinder is filled with a gas. In that way, no optical alignment perturbation is observed up to a gas pressure of 10 bar (see below). The HFC has a finesse varying from 67,000 to 146,000 depending on the wavenumber.

In this work, three fibered Distributed Feedback (DFB) laser diodes from Eblana Photonics Ltd were used as light source. These laser diodes, including a double optical isolation stage and a thermo electrical cooler, are centered at 5704, 5733 and 5785 cm^{-1} (see Fig. 1). By changing the temperature of the diode between 0 °C and 50 °C and keeping the current fixed at 120 mA, the achieved tuning range is between 18.8 and 23.6 cm^{-1} depending of the laser diode. The laser beam is sent into the HFC through a fibered acousto-optic modulator (AOM) (insertion losses of 4 dB at 1705 nm, $f_{AOM}=100.5$ MHz). To generate the ring down (RD) events the cavity length is modulated with a triangular voltage ramp applied to the PZT with amplitude sufficient to cover a little bit more than one free spectral range of the HFC. Each time a longitudinal mode falls in coincidence with the laser frequency, light is transmitted through the cavity and detected with an extended InGaAs photodiode followed by a trans-impedance amplifier (bandwidth 1 MHz). When the photodiode signal is higher than a user-defined threshold, the AOM quickly switches off the laser beam and a RD event is detected. For the evacuated cavity, the measured RD times varied from 20 μs at 5960 cm^{-1} to 10 μs at 5700 cm^{-1}. Absorption spectra were recorded with spectral steps of typically 0.04 cm^{-1} for the highest pressures and 0.007 cm^{-1}

for the lowest ones. About 30 RDs were averaged per spectral points leading to a minimum detectable absorption coefficient (evaluated as the rms of the baseline fluctuation), α_{min}, between 7×10^{-10} cm^{-1} and 1.7×10^{-9} cm^{-1} depending on the RD time.

For each diode, the cell was first filled with pure carbon dioxide (Air Liquide N48, 99.998% stated purity) at a maximal pressure around 10 bar and a series of spectra was then recorded for a ten of pressure values. Fig. 2 shows the evolution of the spectrum with the density up to 8.6 amagat, in the region of the R branch head of the 00031–10002 band. The pressure was measured with a 10 bar pressure transmitter from STS AG (0.1% accuracy full scale). Spectra with the cell evacuated were also recorded before and/or after each series of measurements to obtain the base line. As the ideal gas law is no longer valid for the pressures used in this work it is more appropriate to speak in terms of molecular density instead of pressure. The CO_2 density values were obtained using a model provided by the National Institute of Standards and Technology (http://webbook.nist.gov/chemistry) based on the virial expansion up to the third virial coefficient [17]. The correction reaches ~5% for the highest pressure (7600 Torr).

The gas temperature was determined to be 295 ± 1 K from the rotational structure of the 00031–10002 hot band.

As the continuum absorption is determined from the increase of the CRDS loss rates when the cell is filled with CO_2, it is necessary to insure that the variation of the pressure does not affect the base line of the spectra [18]. This was checked by filling the CRDS cell with pure argon up to 10 bar and monitoring the base line level at a fixed frequency near 5738.4 cm^{-1}. The base line level was observed to increase linearly with pressure with a slope of 10.4×10^{-10} cm^{-1} atm^{-1}. This loss rate is interpreted as being due to Rayleigh scattering of argon for which the calculated loss rate is 9.5×10^{-10} cm^{-1} atm^{-1} [19,20]. Thus filling the cell up to 10 bar does not modify the optical alignment more than the 10^{-10} cm^{-1} level. In addition the base line must remain stable during the recordings. From the different base lines recorded with an empty cell, a temporal stability better than 5×10^{-9} cm^{-1} was obtained for the whole period of measurements. These values are weak and mostly negligible compared to the CO_2 CA on the order of 10^{-7} cm^{-1} level at 10 bar (see below).

2.2. Spectra calibration

The power of the laser sources (~5 mW) and the relatively high insertion losses of the AOM in the studied spectral region prevented us to perform in parallel spectra recordings and laser frequency measurements with the wavemeter at disposal (High-Finesse WSU7-IR, operating range from 630 nm to 1750 nm). Nevertheless, the frequency dependence of the light emitted by the three DFB sources, $\nu_{diode}(T)$, could be measured *versus* the temperature of the diode laser by injecting the totality of the emitted light into the wavemeter. The repeatability of the function was carefully checked from spectrum to spectrum and from day to day for each laser diode. In order to perform an absolute calibration of the frequency scale, the $\nu_{diode}(T)$ function was then refined using spectra recorded at low pressure and accurate CO_2 and H_2O (due to out gassing) line positions provided in the CDSD [5] and HITRAN2012 [21] databanks, respectively.

As an illustration of the temporal stability of the frequency scanning *versus* T, we report in Fig. 3 the determination of the self-pressure shift of a number of R-branch transitions of the 00031–10002 hot band near 5700 cm^{-1}. The linear pressure dependences obtained for these transitions and for a relatively strong and well isolated line of water vapor near 5709.25 cm^{-1} confirm that the stability of the frequency calibration of our spectra is at the 10^{-3} cm^{-1} level.

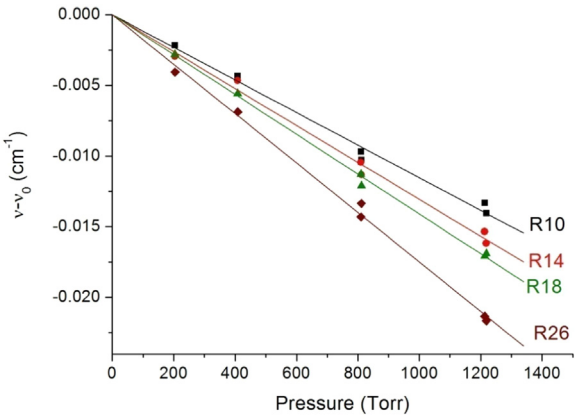

Fig. 3. Self-pressure shift for a few R-branch transitions of the 00031–10002 hot band near 5700 cm^{-1} obtained from the fitted line centers. Note that for the 800 Torr and 1200 Torr total pressure two data points are plotted corresponding to spectra recorded at two different days and showing the good temporal stability of the diode scanning function.

3. List of rovibrational lines

The continuum retrieval requires subtracting the LL contribution. The Carbon Dioxide Spectroscopic Databank (CDSD) [22] which mostly reproduces the HITRAN2012 database [21] in the region was found to have some deficiencies. Thus the first step of the spectra treatment was to construct a satisfactory list of rovibrational lines for natural CO_2 in the 5650–5850 cm^{-1} spectral

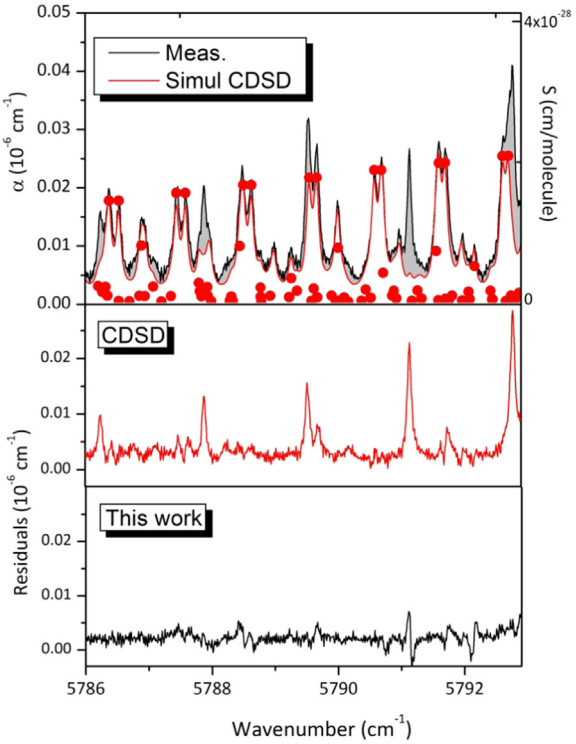

Fig. 4. *Upper panel*: CRDS spectrum of CO_2 near 5790 cm^{-1} recorded at 406 Torr (black line) compared to a spectrum simulation based on CDSD (red solid line). Transitions included in CDSD line list are indicated (red circles). *Middle panel*: Residuals after subtraction of the local line contribution, α_{LL}, calculated with CDSD data base (red solid line). The main features are due to the 41104-00001 band with intensities strongly underestimated in CDSD. *Lower panel*: Residuals after subtraction of the local line contribution, α_{LL}, calculated with the Ames-CDSD composite list adopted in this work (black solid line). (For interpretation of the references to color in this figure legend, the reader is referred to the web version of this article.)

range. In the considered region, the CDSD list and the CRDS spectra agree in general but the CDSD intensity distribution of the relatively strong 41104-00001 band near 5830 cm^{-1} differs strongly from the observation, for instance the measured P branch line intensities are between one and two orders of magnitude larger than the CDSD values as shown in Fig. 4. The effective dipole moment parameters used to calculate the CDSD intensities of the 4110*i*-00001 (i=1–5) sub series of bands were fitted to a small number of measured intensities mostly belonging to the R branch [23]. It turned out that the fitted parameters have bad extrapolation properties and the calculated intensities of the P and Q branches are very imprecise. In that situation, we took advantage of the recent progress achieved by *ab initio* calculations of the CO_2 absorption spectrum [24–27] to construct an improved list for CO_2 in the region. The *ab initio* list computed at NASA Ames [24,25] or University College London [26,27] are theoretical line lists computed using an *ab initio* dipole moment surface and an empirically refined potential energy surface. They have the advantage to be complete and to provide very good line intensities but *ab initio* line positions do not reach the experimental accuracy. Thus, an improved line list, available on request, was obtained in this work by transferring the experimental accuracy on line positions to the *ab initio* line lists using the effective Hamiltonian calculations as developed for CDSD. This approach was previously followed by Zak et al. for the main isotopologue up to 8000 cm^{-1} [26] and will be used to generate the CO_2 list in the new version of the HITRAN database. Rovibrational quantum numbers were attached to the Ames transitions between 5650 and 5850 cm^{-1} and the corresponding positions calculated within the effective Hamiltonian approach [5] were substituted to the *ab initio* positions. Self-broadening, γ_{self}, and self-pressure shift, δ_{self}, coefficients obtained by complex Robert-Bonamy (CRB) calculations [28] were attached to the different transitions. Fig. 4 presents the differences between the experimental spectrum near 5790 cm^{-1} and simulations based on the CDSD list and the Ames-CDSD composite list. The agreement obtained with this latter list is very satisfactory confirming the accuracy of Ames intensities at the level of the experimental noise of our spectra.

We took advantage of the low pressure spectra at disposal to test the line profile parameters included in our list using the R-branch transitions of the 00031–10002 hot band near 5700 cm^{-1}. Spectra at 200, 400, 800 and 1200 Torr were reproduced by a multiline fit using a Voigt profile for the line shape. The δ_{self} and γ_{self} coefficients were obtained from a linear fit of the line centers and Lorentzian line widths of the *R*(8)-*R*(30) lines *versus* pressure, respectively (see Fig. 3 and Table 1). The comparison to the results of the CRB calculations [28] displayed in Fig. 5 shows an agreement at the % level for the broadening coefficient. Nevertheless, the rotational

Table 1
Measured self-broadening and pressure shift coefficients for transitions of the R-branch of the 00031–10002 band of $^{12}C^{16}O_2$. Values given in parenthesis correspond to 1σ uncertainty of the linear fit versus P in units of the last digit.

Transition	γ_{self} (cm^{-1} atm^{-1})	δ_{self} (cm^{-1} atm^{-1})
R10	0.1080(5)	−0.0088(5)
R12	0.1058(6)	−0.0091(7)
R14	0.1039(5)	−0.0099(5)
R18	0.1010(4)	−0.0107(3)
R20	0.0993(3)	−0.0110(3)
R22	0.0983(2)	−0.0126(10)
R24	0.0966(4)	−0.0129(8)
R26	0.0947(5)	−0.0133(4)
R28	0.0936(4)	−0.0143(12)
R30	0.0916(2)	−0.0148(10)
R32	0.0900(1)	

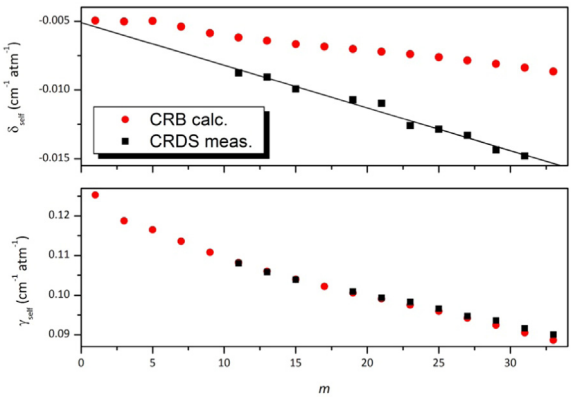

Fig. 5. Rotational dependence of the measured and calculated self-broadening (bottom) and self-pressure shift- (top) coefficients of the R-branch of the 00031–10002 band. m=J+1 for the R-branch. CRB means Complex Robert Bonamy [28].

dependence of the self-pressure shift coefficients is found significantly stronger than predicted. The amplitude of δ_{self} is varying linearly with m (=J+1) with a slope about twice large as predicted and the value at m= 1 is very close to the CRB value. The slope in the line shifts *versus* J from the CRB calculations came from adjusting to the data of Devi et al. [29]. From comparison with other data sets, it now appears that the Devi et al. data for the line shift may not decrease quickly enough with increasing J. This dependence will be studied in a future work. Consequently, we replaced the δ_{self} coefficients of the *R* branch of the 00031–10002 band in the Ames-CDSD list by their empirical value obtained from $\delta_{self} = -0.0051 - 3.1 \times 10^{-4}\, m$ cm^{-1} atm^{-1}.

4. Data analysis and retrieved binary coefficients

The measured extinction coefficient (in cm^{-1}) can be expressed as a sum of three terms:

$$\alpha(\nu) = \frac{1}{c\tau(\nu)} - \frac{1}{c\tau_0(\nu)} = \alpha_{LL} + \alpha_{CA} + \alpha_{Ray} \quad (1)$$

where τ and τ_0 correspond to the ring down times when the cell is filled and evacuated, respectively. α_{LL} and α_{CA} are the contributions due to the CO_2 local lines (LL) and the continuum absorption (CA), respectively, and α_{Ray} is the Rayleigh scattering losses of CO_2. In Eq. (1) we neglected the small differences from unity ($< 5 \times 10^{-3}$) of the CO_2 refractive index.

For each series of recordings, corresponding to a given DFB diode laser, the spectra were first corrected from the zero-pressure baseline, $1/c\tau_0(\nu)$, obtained with the empty cell and modeled by a cubic spline polynomial function *versus* the frequency.

4.1. Rayleigh scattering

The extinction due to Rayleigh scattering which is proportional to the gas density, was subtracted. The Rayleigh scattering cross-section was calculated from the refractive index, n, using Eq. (1) of Ref. [19]. We determined the CO_2 refractive index at 5738.55 cm^{-1} from the longitudinal modes scrolling with pressure using our CRDS set-up. A value of 1.000402 was measured for 1 atm at room temperature and was adopted for all the diodes as n is expected to vary by no more than 10^{-6} over our spectral range [30]. Our value agrees within 2% with the refractive indexes reported in [30] and in [19]. Rayleigh scattering losses lead to a small but non negligible contribution to the extinction of 2.7×10^{-9} cm^{-1} $amagat^{-1}$.

4.2. CO_2 LL contribution

The choice of the line profile to describe the monomer contribution deserves to be discussed as it has a direct impact on the CA retrieved values. Far from the line or band center, the impact approximation, where the collision duration can be neglected, is not valid and non-Voigt behavior of the far wings is expected [2]. An empirical approach consists in using a χ-factor, varying with the distance to the line center, to modify (generally to reduce) the Voigt profile into the wings. Several examples of this χ-factor approach have been proposed for CO_2 [4,31,32]. Note that χ-factors are band-dependent and their extrapolation to other bands (or spectral regions) may lead to inaccuracies. An extreme case of this approach consists in truncating the Voigt or Lorentzian profile at a given distance from the line center. This is what is generally adopted to retrieve the water vapor continuum [33]: a Lorentzian profile truncated at $\pm 25\ cm^{-1}$ from the line center and reduced by the pedestal value at $25\ cm^{-1}$ is used to simulate the water monomer contribution. In this work we adopted the same approach with a Voigt profile by analogy with the water vapor continuum and because at $25\ cm^{-1}$ from the line center, the impact approximation is valid over a large part of our pressure range. It is important to keep in mind that in general, the retrieved value of the continuum depends on the choice of the LL profile and of the database of the monomer. The impact of the choice of the line profile on the retrieved CA is discussed in Section 5.

4.3. H_2O LL contribution

Water vapor absorption lines are present in our spectra as a result of out gassing from the walls of the cell. Maximum relative concentration of 100 ppm was determined for the lowest total pressure while the partial pressure was always below 50 mTorr. As some of the water vapor transitions in the studied spectral range have intensities of the order of 5×10^{-23} cm/molecule, i.e. three orders of magnitude larger than the strongest CO_2 lines in the region, their contributions were subtracted from the measured extinction coefficient. HITRAN2012 line list [21] was used to calculate the water vapor contribution with the same truncated profile as the one used for CO_2. In the HITRAN water line list, the air-broadening and shift coefficients were replaced by the CO_2–broadening, γ_{CO_2}, and shift, δ_{CO_2}, coefficients obtained by CRB calculations [34]. Again for the strongest water vapor lines calculated δ_{CO_2} values were replaced by the measured ones.

4.4. Line-mixing effect

In our pressure conditions, lines cannot be considered as collisionally isolated and the well-known collisional line-mixing (LM) occurs leading to significant changes of the absorption spectrum [2]. Here, this effect was taken into account through the use of the impact and Energy Corrected Sudden approximations, as done in Ref. [31]. Note that this approach is valid in the center and near wing regions where the impact approximation holds. The package provided in [31] and updated in [15] was used here to calculate the absorption spectrum. For the considered spectral region, spectroscopic data of this package were replaced by data of the above constructed Ames-CDSD line list. The parameters of the models were also slightly modified in order to better match the observed spectra.

The LM correction was then determined by the difference between a spectrum simulated including LM effects and a simple sum of (non-truncated) Voigt profiles. Fig. 6 illustrates the impact of the LM effects in the region around $5700\ cm^{-1}$ where the R branch of the 00031–10002 band dominates. The inclusion of LM effects allows a much better reproduction of the spectrum but some

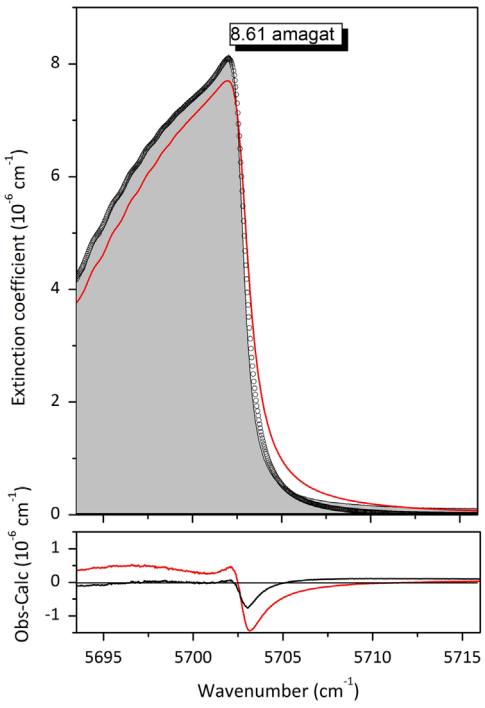

Fig. 6. Impact of the line-mixing in the region of the R branch of the 00031–10002 band. Upper panel: CRDS spectrum, recorded for a density of 8.61 amagat (open circles) compared to the spectra simulations of the CO_2 lines with (light grey) and without (red solid line) the line mixing effects. Lower panel: corresponding (Obs.–Sim.) residuals after subtraction of these contributions. (For interpretation of the references to color in this figure legend, the reader is referred to the web version of this article.)

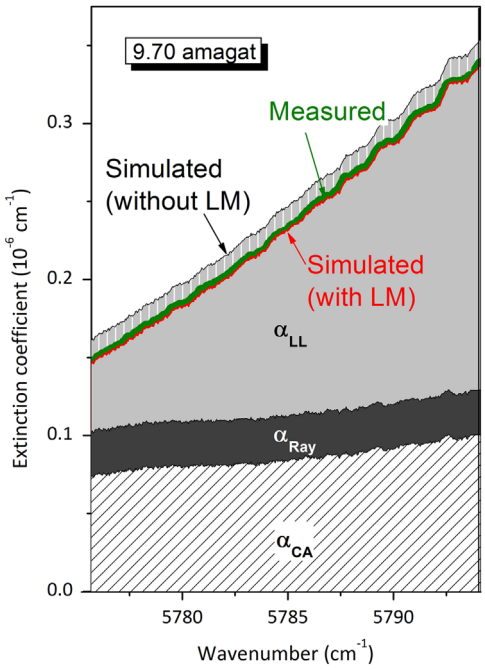

Fig. 7. The different contributions to the CO_2 extinction coefficient near $5785\ cm^{-1}$ recorded with a density of 9.70 amagat. The simulated spectrum with LM (red line) matches very well the measured extinction (green circles). Note the negative contribution of the LM. (For interpretation of the references to color in this figure legend, the reader is referred to the web version of this article.)

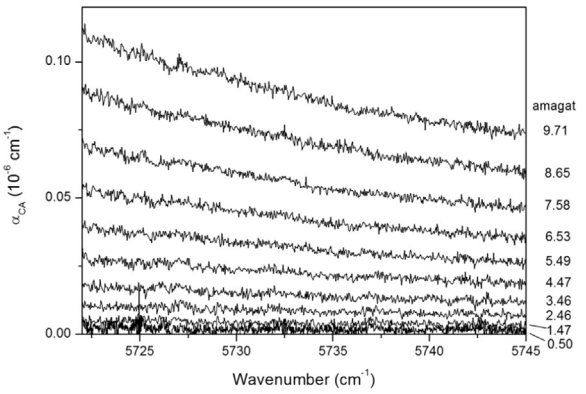

Fig. 8. CO_2 continua retrieved from the series of spectra recorded at different densities with the 1744 nm laser diode.

significant deviations are still noted near the R branch band head.

The continuum absorption, α_{CA}, is the residuals of the measured extinction after subtraction of Rayleigh scattering losses, LL absorption contributions of CO_2 and H_2O and the LM correction. The CA retrieval around 5785 cm^{-1} presented on Fig. 7 shows that, in this spectral interval, the LL contribution is very well reproduced and that the LM correction is limited and negative.

4.5. Binary absorption coefficients

For a given wavenumber, the density dependence of the continuum is expected to be purely quadratic with a proportionality factor called the binary absorption coefficient, expressed in cm^{-1} $amagat^{-2}$. The procedure described above was applied to each series of spectra recorded with the 3 laser diodes at different densities. An example of a series of retrieved continua is shown on Fig. 8 for the 1744 nm laser source (5722–5745 cm^{-1}). As illustrated in Fig. 9, the density dependence of the retrieved CA was found to be purely quadratic for the recordings performed with the low frequency diode laser below 5720 cm^{-1} but above this value, there is evidence of a small but significant linear contribution. Several determinations in the $5722-5794\ cm^{-1}$ range indicate that the linear contribution varies between 1.2×10^{-9} and 2.0×10^{-9} cm^{-1} $amagat^{-1}$ i.e. around 20% of the CA value at 9.7 amagat. The linear contribution cannot be explained by uncertainty on the Rayleigh scattering losses (which were subtracted) because its amplitude would require an increase of 40% and more of the Rayleigh losses [19] which is much larger than the uncertainty on the Rayleigh scattering coefficient estimated to be a few percents (see above). A tentative explanation could be that, in spite of the low concentration of water vapor in our samples, this small linear increase is caused by the water vapor foreign-continuum. This latter designates here the continuum absorption due to interactions between water molecules (present as trace species in our spectra) and CO_2 molecules which is proportional to the product of the CO_2 and water vapor densities. In order to estimate the order of magnitude of this type of contribution we adopted the cross-section value of 1.7878×10^{-25} cm^2 $molecule^{-1}$ at 5730 cm^{-1} given in the MT_CKD V2.8 model [33] for the foreign-water vapor continuum at 296 K which, in this case, corresponds to interactions between water molecules and air. Using the water vapor partial pressure, retrieved from the fit of the water lines in the recorded spectra, we obtain an almost linear contribution of 2.6×10^{-10} cm^{-1} $amagat^{-1}$ for the diode emitting around 5730 cm^{-1}. This value corresponds to about 10 and 20% of the linear term contribution to the CA at 9.7 amagat. It is worth noting that for the low energy DFB diode laser centred around 5700 cm^{-1}, water vapor relative concentration is smaller and the fact that the pressure dependence was found purely quadratic in this spectral interval (Fig. 9) gives some credit to the interpretation of the linear term as due to a water vapor foreign-continuum. Specific experiments devoted to this issue should be undertaken to clarify the origin of the linear term.

The binary coefficient over the whole studied spectral range was obtained from the highest density recordings after subtraction of a mean linear contribution of 1.5×10^{-9} cm^{-1} $amagat^{-1}$ above 5720 cm^{-1}. The frequency dependence of the binary coefficient is presented in Fig. 10. A smooth dependence with wavenumber is observed with a minimum value of 6×10^{-10} cm^{-1} $amagat^{-2}$.

5. Discussion

5.1. Uncertainties on the retrieved binary coefficients

As mentioned above, the base line stability is an important prerequisite to accurately measure weak CA. From our measurements a temporal stability better than 5×10^{-9} cm^{-1} is observed during the whole measurements period. A standard deviation better than 8×10^{-10} cm^{-1} was found (Fig. 9), showing that for a series of recordings over a few hours the achieved stability is particularly good (for comparison, the CA level at 9.7 amagat is on the order of 10^{-7} cm^{-1}). Consequently, the base line instability is not believed to be an important error source.

As mentioned above the uncertainty related to Rayleigh

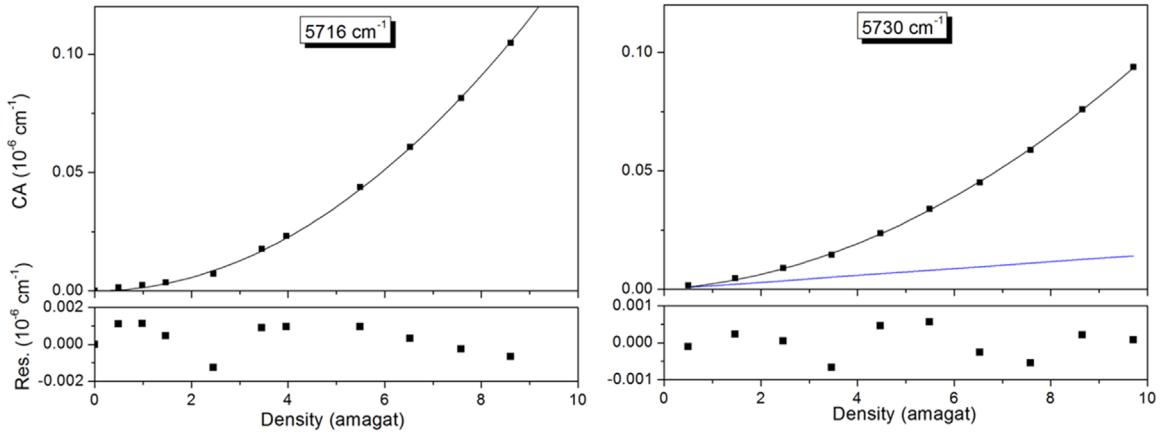

Fig. 9. Density dependence of the continuum absorption at 5716 and 5730 cm^{-1} (upper panels) and corresponding residuals (lower panels) after subtraction of the fitted quadratic polynomial. At 5716 cm^{-1}, the fit uses a purely quadratic function while a linear term (blue line) is included in the fit at 5730 cm^{-1}. (For interpretation of the references to color in this figure legend, the reader is referred to the web version of this article.)

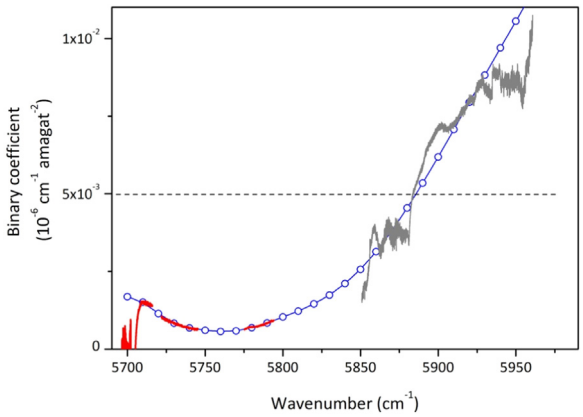

Fig. 10. Overview of the binary coefficient retrieved at room temperature from CRDS spectra recorded in this work (red line) and reported in Ref. [14] (grey line). The blue open circles represent the approximate function recommended for the CO_2 binary coefficient in the region. The dashed line corresponds to the constant value used in Ref. [9] to obtain the best fit of the Venus spectra for the 1.74 μm window. (For interpretation of the references to color in this figure legend, the reader is referred to the web version of this article.)

scattering, known at the 2% level of the CA, is also negligible. A larger error source could come from the subtraction of the LL contribution of the CO_2 monomer. Two aspects have to be considered: the LL database and the profile associated to each line for the LL simulation. As shown in Fig. 4, the constructed Ames-CDSD line list was found to satisfactorily account for the LL lines. The CRB calculated self-broadening coefficients were validated by those we measured in the *R*-branch of the 00031–10002 band. The discrepancy observed for the self-pressure-shift coefficients has no real impact on the retrieved CA which varies slowly with the wavenumber. Overall, inaccuracies due to the CO_2 and H_2O line lists are thus expected to have a marginal impact on the retrieved CA values.

To quantify the impact of the line profile, we performed simulations of the CO_2 contribution at 7600 Torr for the different χ-factor profiles of Refs. [4,31,32] and compare them to the simulation using a $\pm 25\ cm^{-1}$ truncated profile. In the 5745–5795 cm^{-1} spectral range, the obtained differences are limited to ~5% or less of the retrieved CA. At lower wavenumber, they can reach 20% of the continuum (at 5720 cm^{-1}). Note that, strictly speaking, the choice of the profile and LL database adopted to calculate the monomer contribution should not be considered as an uncertainty as far as the CA retrieval is traceable.

Finally, considering the observed linear contribution, possibly due to a contribution of foreign continuum, the apparent 15% discontinuity between the binary coefficients obtained for the two lower energy DFB diode lasers (Fig. 10), the global uncertainty on the retrieved binary coefficients is estimated to be on the order of 30% (1σ).

5.2. Comparison with previous literature data

To our knowledge, the only measurements of CO_2 CA available in the 1.74 μm window are those we reported in Ref. [15] for the 5850–5960 cm^{-1} spectral range just above the region investigated in this work. The corresponding binary coefficients show a frequency dependence which is consistent with the present results (see Fig. 10). A strong decrease from 1×10^{-8} cm^{-1} $amagat^{-2}$ at 5960 cm^{-1} to 6×10^{-10} cm^{-1} $amagat^{-2}$ for 5750 cm^{-1} is observed. We note that the constant value of 5×10^{-9} cm^{-1} $amagat^{-2}$ adopted in [9] to model Venus spectra over the whole 1.74 μm window is about the average value in the region. Let us mention that the value retrieved at the center of the window is not far to the value of 5.5×10^{-10} cm^{-1} $amagat^{-2}$ retrieved around 8475 cm^{-1} corresponding to the center of the 1.18 μm window [14].

For the convenience of potential users, we adjusted a smooth function reproducing the binary coefficients over the 5700–5950 cm^{-1} interval (Fig. 10). The recommended binary coefficients are provided in Table 2 with a 10 cm^{-1} step.

6. Concluding remarks

The spectra of CO_2 in the 1.74 μm window were recorded at different pressures with a CRDS cell specially designed for high pressure measurements [15]. Three DFB laser diodes were used to characterize the most transparent interval of the window (5693–5795 cm^{-1}). The sensitivity of the recordings revealed some inaccuracies of the HITRAN2012 and CDSD databases concerning the 41104-00001 band which is a weak band (intensities on the order of 10^{-28}–10^{-27} cm/molecule) but has a strong relative contribution in the region. In order to satisfactorily subtract the LL contribution, a composite line list was built using the CDSD and Ames databases for the positions and intensities, respectively, and self-broadening and pressure shift coefficients calculated with the CRB method. This line list was carefully validated using the recorded spectra. The CA was retrieved after subtraction of the CO_2 monomer contribution and a Voigt profile truncated at $\pm 25\ cm^{-1}$ from the center of each line. LM effects which play an important role in the region of the 00031–10002 band near 5700 cm^{-1} were taken into account using the relaxation matrix *W* and the impact and Energy Corrected Sudden approximations. Rayleigh scattering and water monomer contributions were also evaluated and subtracted. The CA values retrieved up to 9.7 amagat from the recordings performed with the lower frequency laser diode below 5720 cm^{-1}, showed a purely quadratic pressure dependence. For the recordings performed with the two higher frequency laser diodes above 5720 cm^{-1}, the density dependence of the retrieved CA showed a small, $\sim 1.5 \times 10^{-9}$ cm^{-1} $amagat^{-1}$, linear dependence. We tentatively explain this linear contribution as due to the foreign water continuum as trace of water vapor were present in the sample used for the recordings above 5720 cm^{-1}.

Including our previous results of Ref. [14], we provide a set of the CO_2 binary coefficients at room temperature for the entire 5690–5950 cm^{-1}. Strong frequency dependence between 1×10^{-8} cm^{-1} $amagat^{-2}$ at 5960 cm^{-1} and 6×10^{-10} cm^{-1} $amagat^{-2}$ at the center of the 1.74 μm window is noted. The constant value of 5×10^{-9} cm^{-1} $amagat^{-2}$ used to analyze Venus spectra is close to the average value in the region adopted in [9]. Let us underline

Table 2
Recommended binary coefficients (in 10^{-10} cm^{-1} $amagat^{-2}$) obtained from a smooth function adjusted to the experimental data (see Fig. 10).

Wavenumber (cm^{-1})	**5700**	**5710**	**5720**	**5730**	**5740**	**5750**	**5760**	**5770**	**5780**	**5790**	**5800**
Binary coefficient	16.9	15.1	11.5	8.4	6.8	6.0	5.7	5.8	6.9	8.4	10.3
Wavenumber (cm^{-1})	**5810**	**5820**	**5830**	**5840**	**5850**	**5860**	**5870**	**5880**	**5890**	**5900**	**5910**
Binary coefficient	12.2	14.5	17.4	21.1	25.7	31.3	38.0	45.4	53.4	61.9	70.7
Wavenumber (cm^{-1})	**5920**	**5930**	**5940**	**5950**	**5960**						
Binary coefficient	79.4	88.2	97.0	105.6	114.3						

that the temperature dependence of the CO_2 continuum is unknown which is a drawback to apply the present results to Venus spectra. The development of CRDS set ups allowing for both high temperature and high pressure spectroscopy is an experimental challenge highly desirable to really quantify the CA at temperature matching the conditions encountered in the Venusian atmosphere. Finally, we note that if the water vapor foreign continuum origin of the observed linear contribution to CA is confirmed, its impact may also be considered in Venus spectra as water vapor is present at the 30 ppm level in the Venus' atmosphere [13]. This value is on the same order of magnitude as the water vapor concentration in our recordings.

Acknowledgments

The support of the Laboratoire International Asssocié SAMIA between CNRS (France) and RAS (Russia) is acknowledged. This work was performed in the frame of the LabexOSUG@2020 (ANR10 LABX56). PC thanks CNRS and Université Grenoble Alpes for three-month support at LIPhy-Grenoble and the Scientific Grant Agency of Slovak Republic (Project No. 1/0903/17). The work of SAT is partly supported by the Government of the Russian Federation in frame of contract No. 02.A03.21.0006, Act 211. Research performed at the University of Massachusetts Lowell is supported by the National Science Foundation through Grant No. AGS-1622676.

References

[1] Bézard B, de Bergh C. Composition of the atmosphere of Venus below the clouds. J Geophys Res 2007;112:E04S07.
[2] Hartmann JM, Boulet C, Robert D. Collisional effects on molecular spectra: laboratory experiments and models, consequences for applications. Elsevier; 2008.
[3] Frommhold L. Collision-induced absorption in gases. Cambridge: Cambridge University Press; 1993 and 2006.
[4] Tonkov MV, Filippov NN, Bertsev VV, Bouanich JP, Van Thanh Nguyen, Brodbeck C, Hartmann J-M, Boulet C, Thibault F, Le Doucen R. Measurements and empirical modelling of pure CO_2 absorption in the 2.3 μm region at room temperature: far wings, allowed and collision-induced bands. Appl Opt 1996;35:4863–4870.
[5] Tashkun SA, Perevalov VI, Gamache RR, Lamouroux J. CDSD-296 high resolution carbon dioxide spectroscopic databank: version for atmospheric applications. J Quant Spectrosc Radiat Transf 2015;152:45–73.
[6] Rothman LS, Gordon IE, Barber RJ, Dothe H, Gamache RR, Goldman A, Perevalov V, Tashkun SA, Tennyson J. HITEMP, the high-temperature molecular spectroscopic database. J Quant Spectrosc Rad Transf 2010;111:2139–2150.
[7] Filippov NN, Asfin RE, Sinyakova TN, Grigoriev IM, Petrova TM, Solodov AM, Solodov AA, Buldyreva JV. Experimental and theoretical studies of CO_2 spectra for planetary atmosphere modelling: region 600–9650 cm^{-1} and pressures up to 60 atm. Phys Chem Chem Phys 2013;15:13826–13834.
[8] Stefani S, Piccioni G, Snels M, Grassi D, Adriani A. Experimental CO_2 absorption coefficients at high pressure and high temperature. J Quant Spectrosc Radiat Transf 2013;117:21–28.
[9] De Bergh C, Bézard B, Crisp D, Maillard JP, Owen T, Pollack J, Grinspoon D. Water in the deep atmosphere of Venus from high-resolution spectra of the night side. Adv Space Res 1995;15:79–88.
[10] Marcq E, Encrenaz T, Bézard B, Birlan M. Remote sensing of Venus' lower atmosphere from ground-based IR spectroscopy: latitudinal and vertical distribution of minor species. Planet Space Sci 2006;54:1360–1370.
[11] Pollack JB, Dalton JB, Grinspoon D, Wattson RB, Freedman R, Crisp D, Allen DA, Bézard B, De Bergh C, Giver LP, Ma Q, Tipping R. Near-infrared light from Venus' nightside: a spectroscopic analysis. Icarus 1993;103:1–42.
[12] Seiff A, Schofield JT, Kliore AJ, Taylor FW, Limaye SS, Revercomb HE, Sromovsky LA, Kerzhanovich VV, Moroz VI, Marov MY. Models of the structure of the atmosphere of Venus from the surface to 100 km altitude. Adv Space Res 1985;5:3–58.
[13] Bézard B, Tsang CC, Carlson RW, Piccioni G, Marcq E, Drossart P. Water vapor abundance near the surface of Venus from Venus Express/VIRTIS observations. J Geophys Res 2009;114:E00B39.
[14] Snels M, Stefani S, Piccioni G, Bézard B. Carbon dioxide absorption at high densities in the 1.18 μm night side transparency window of Venus. J Quant Spectrosc Radiat Transf 2014;133:464–471.
[15] Kassi S, Campargue A, Mondelain D, Tran H. High pressure cavity ring down spectroscopy: application to the absorption continuum of CO_2 near 1.7 μm. J Quant Spectrosc Radiat Transf 2015;167:97–104.
[16] Mondelain D, Vasilchenko S, Čermák P, Kassi S, Campargue A. The CO_2 absorption spectrum in the 2.3 μm transparency window by high sensitivity CRDS: (ii) self-absorption continuum. J Quant Spectrosc Radiat Transf 2017;187:38–43.
[17] Lemmon E, McLinden M, Friend D. Thermophysical properties of fluid systems. in: NIST chemistry webbook, NIST standard reference database number 69. Gaithersburg, MD: National Bureau of Standards and Technology; 2012.
[18] Campargue A, Kassi S, Mondelain D, Vasilchenko S, Romanini D. Accurate laboratory determination of the near-infrared water vapor self-continuum: a test of the MT_CKD model. J Geophys Res Atmos 2016;121:13180–13203.
[19] Thalman R, Zarzana KJ, Tolbert MA, Volkamer R. Rayleigh scattering cross-section measurements of nitrogen, argon, oxygen and air. J Quant Spectrosc Radiat Transf 2014;147:171–177.
[20] Thalman R, Zarzana KJ, Tolbert MA, Volkamer R. Erratum to "Rayleigh scattering cross-section measurements of nitrogen, argon, oxygen and air" J Quant Spectrosc Radiat Transf 147; 2014. pp. 171–177. J Quant Spectrosc Radiat Transf; 2017. pp. 189:281–282.
[21] Rothman LS, Gordon IE, Babikov Y, Barbe A, Benner DC, Bernath PF, et al. The HITRAN2012 molecular spectroscopic database. J Quant Spectrosc Radiat Transf 2013;130:4–50.
[22] Tashkun SA, Perevalov VI, Gamache RR, Lamouroux J. CDSD-296 high resolution carbon dioxide spectroscopic databank: version for atmospheric applications. J Quant Spectrosc Radiat Transf 2015;152:45–73.
[23] Perevalov BV, Campargue A, Gao B, Kassi S, Tashkun SA, Perebalov VI. New CW-CRDS measurements and global modeling of $^{12}C^{16}O_2$ absolute line intensities in the 1.6 μm region. J Mol Spectrosc 2008;252:190–197.
[24] Huang X, Freedman RS, Tashkun SA, Schwenke DW, Lee TJ. Semi-empirical $^{12}C^{16}O_2$ IR line lists for simulations up to 1500 K and 20,000 cm^{-1}. J Quant Spectrosc Radiat Transf 2013;130:134–146.
[25] Huang X, Gamache RR, Freedman RS, Schwenke DW, Lee TJ. Reliable infrared line lists for 13 CO_2 isotopologues up to E = 18,000 cm^{-1} and 1500 K, with line shape parameters. J Quant Spectrosc Radiat Transf 2014;147:134–144.
[26] Zak E, Tennyson J, Polyansky OL, Lodi L, Zobov NF, Tashkun SA, Perevalov VI. A room temperature CO_2 line list with ab initio computed intensities. J Quant Spectrosc Radiat Transf 2016;177:31–42.
[27] Polyansky OL, Bielska K, Ghysels M, Lodi L, Zobov NF, Hodges JT, et al. High accuracy CO_2 line intensities determined from theory and experiment. Phys Rev Lett 2015;114:243001.
[28] Lamouroux J, Gamache RR, Laraia AL, Hartmann J-M, Boulet C. Semiclassical calculations of half-widths and line shifts for transitions in the 30012 – 00001 and 30013 – 00001 bands of CO_2. III: self collisions. J Quant Spectrosc Radiat Transf 2012;113:1536–1546.
[29] Devi VM, Benner DC, Brown LR, Miller CE, Toth RA. Line mixing and speed dependence in CO_2 at 6348 cm^{-1}: positions, intensities, and air- and self-broadening derived with constrained multispectrum analysis. J Mol Spectrosc 2007;242:90–117.
[30] Old J, Gentili K, Peck E. Dispersion of carbon dioxide. J Opt Soc Am 1971;61:89–90.
[31] Tran H, Boulet C, Stefani S, Snels M, Piccioni G. Measurements and modelling of high pressure pure CO_2 spectra from 750 to 8500 cm^{-1}. I-central and wing regions of the allowed vibrational bands. J Quant Spectrosc Radiat Transf 2011;112:925–936.
[32] Bézard B, Fedorova A, Bertaux JL, Rodin A, Korablev O. The 1.10 and 1.18 μm night side windows of Venus observed by SPICAV-IR aboard Venus Express. Icarus 2011;216:173–183.
[33] Mlawer EJ, Payne VH, Moncet J, Delamere JS, Alvarado MJ, Tobin DC. Development and recent evaluation of the MT_CKD model of continuum absorption. Philos Trans R Soc A 2012;370:2520–2556.
[34] Gamache RR, Farese M, Renaud C. A spectral line list for water isotopologues in the 1100–4100 cm^{-1} region for application to CO_2-rich planetary atmospheres. J Mol Spectrosc 2016;326:144–150.